DOI:10.1190/image2022-3736085.1

Statistical depth imaging through complex cluttered near surface with path summation

Andrey Bakulin, Ilya Silvestrov, EXPEC Advanced Research Center, Saudi Aramco, Maxim Protasov, Institute of Petroleum Geology and Geophysics, SB RAS*

Summary

We study the problem of imaging deep reflection targets in the presence of a complex land near surface modeled as a random clutter. The synthetic example with random clutter reproduces significant scattering distortions and image defocusing observed in field data from the desert environment. We perform a numerical study of focusing target events in the image domain using various realizations of the cluttered media velocity models. We also perform a feasibility study of statistical imaging with path summation and present a heuristic technique to obtain a subsurface image without specifying a deterministic velocity-depth model.

Introduction

In land seismic exploration, strong scattering caused by small- and medium-scale near-surface heterogeneities strongly deteriorates the quality of depth seismic images Xie et al., 2016; Bakulin et al., 2020). While the imperfections in the migration velocity model cause substantial phase errors preventing the extrapolated wavefield from proper focusing (Xie et al., 2016), accurate reconstruction of all the near-surface complexities is likely out of reach by modern algorithms. Since the near-surface model itself is often not a primary object of interest, a reasonable workaround considers it as some stochastic media (Ikelle et al., 1993). Evaluating and using statistical properties of this media, imaging algorithms might mitigate the near-surface- and overburden-related challenges and produce more accurate images of deep horizons. Several imaging approaches following this idea have been introduced in the past. Borcea et al. (2003) used the concept of time-reversed wave propagation and proposed an interferometric imaging approach to obtain more statistically stable seismic images in random media. Similarly, Sava and Poliannikov (2008) extended conventional cross-correlation migration imaging conditions to achieve better images for models with rapid, small-scale velocity variations in the overburden.

An alternative way for imaging without knowing an exact velocity model was introduced by Landa et al. (2006) based on a concept of path-integral summation. The main idea is to stack all possible images obtained with an ensemble of velocity distributions instead of using a single "best" one as in conventional algorithms. Furthermore, additional weights in the summation are introduced to emphasize the most probable image portions. The ideas of path-integral seismic imaging were explored in several applications in the time domain, including stack to zero offset (Landa, 2004; Keydar, 2005; Yilmaz, 2018), time-migration (Landa et al., 2006), velocity analysis (Schleicher and Costa, 2009; Burnett et al., 2011), and diffraction imaging (Merzlikin and Fomel, 2015; Decker and Fomel, 2019). Extending these ideas to depth imaging is more challenging due to the need to adequately sample the multidimensional space of possible depth velocity models and choose suitable weighting functions for the summation. Some initial results of path-integral seismic imaging in depth are presented by Landa et al. (2005, 2006). Protasov et al. (2017) showed that such an approach provides a possible framework for subsalt imaging without precise knowledge or identifying salt-sediment boundaries.

In this study, we show an initial investigation of the path-summation approach for depth imaging of target deep reflectors in the presence of a complex near-surface scattering layer. We characterize such layer as a random, cluttered medium that remains unknown but whose statistical properties can be guessed or estimated from the data.

Path-summation method and focusing measures

Instead of relying on a chance to reconstruct an exact velocity model (Xie et al., 2016), the idea of the path-summation method is to produce many realizations of the depth model (Landa et al., 2006) that could potentially capture correct fragments of the subsurface velocity. Since each model can only reveal the image of a particular portion of the subsurface, the final image is assembled as a weighted summation of elementary images that let each one contribute a valuable piece to the overall puzzle. In our case of imaging in a desert environment with complex near-surface, it can be done by a weighted summation of individual migrated images computed for different realizations of the near-surface migration velocity model as follows:

$$\boldsymbol{I_w}(\boldsymbol{x}) = \sum_{\boldsymbol{k}} \boldsymbol{w_k}(\boldsymbol{x}) \boldsymbol{I_k}(\boldsymbol{x}) \,, \qquad (1)$$

where $\boldsymbol{I_w}$ is a final image at point $\boldsymbol{x}$, $\boldsymbol{I_k}$ is an image for model realization with index k, and $\boldsymbol{w_k}$ is a weighting function. Such a procedure can be considered a statistical averaging over an ensemble of possible near-surface models. We define the near-surface model realizations using statistical modeling of random anomalies, called clutter. Since the scale of the anomalies of interest is comparable to or less than the dominant source wavelength, we use reverse-time migration (RTM) to tackle them correctly during wave propagation. To simplify the analysis, we consider post-stack RTM in this work, while the results can also be extended to a prestack case.

The summation process is designed in such a way that the most focused image parts provide a maximum contribution

to the final image, whereas less focused parts would be de-emphasized. Therefore we use a focusing weight $\boldsymbol{w_k}$ to define the focusing quality of the corresponding image $\boldsymbol{I_k(x)}$ which is the result of the data migration using model realization $\boldsymbol{m_k(x)}$. We choose the weights as follows:

$$\boldsymbol{w_k(x)} = \frac{\boldsymbol{W_k(x)}}{\sum_k \boldsymbol{W_k(x)}}. \quad (2)$$

Here, $\boldsymbol{W_k}$ is an exponential weighting function following the path-integral approach (Landa et al., 2006):

$$W_k(\boldsymbol{x}) = \exp\left(-\alpha\left(1 - \frac{f_k(x)}{\max_{k,x}(f_k(x))}\right)\right), \quad (3)$$

where $\boldsymbol{\alpha}$ is some scalar, and $\boldsymbol{f_k(x)} = \boldsymbol{f(I_k(x))} \geq 0$ is a focusing measure of image $\boldsymbol{I_k}$ at a point $\boldsymbol{x}$ to be defined later.

The focusing weight (3) includes the normalization of all the elements. This normalization provides scaling, so the weight value varies from zero to one. At the points with good focusing, the intermediate weight $\boldsymbol{W_k}$ is close to one. In contrast, it will tend to zero exponentially at locations with poor focusing. As a result, the most focused image parts should provide a maximum contribution to the final image.

It is necessary to use an appropriate focusing measure f to determine the weights. According to Pertuz et al. (2013), the focusing measures can be divided into several groups: gradient-based operators, laplacian-based operators, wavelet-based operators, statistics-based operators, DCT-based (discrete cosine transform), and miscellaneous operators. Gradient-based and Laplacian-based operators provide measures based on the gradient or first derivatives of the image and correspondingly Laplacian or second derivatives of the image. Wavelet-based and DCT-based operators measure the focus level using the coefficients of the discrete wavelet transform and DCT describing the frequency and spatial content of images. Finally, statistics-based operators take advantage of several image statistics as texture descriptors to compute the focus level. During our investigations for a set of seismic images constructed in the cluttered model, we chose several measures for detailed investigation among the variety of the focusing operators. Based on the numerical results, we propose to use a focus measure based on the spatial frequency operator proposed by Eskicioglu and Fisher (1995):

$$f(\boldsymbol{x}_0) = \sum_{|x-x_0|<\delta} \sqrt{I_x^2(\boldsymbol{x}) + I_z^2(\boldsymbol{x})}, \quad (4)$$

where $\boldsymbol{I_X}$, $\boldsymbol{I_Z}$ are spatial image derivatives.

Numerical simulations

Let us generate a complex near-surface model using random clutter (Figure 1a). More specifically, we add to a homogeneous model a velocity perturbation field described by Gaussian distribution function with two parameters: correlation length, defining the typical size of heterogeneities, and standard deviation, characterizing the magnitude of the velocity perturbation. The true model uses a homogeneous velocity of 2000 m/s, correlation length of 35 m, and a standard deviation of 400 m/s. Synthetic input for imaging is generated by computing zero-offset seismic data via acoustic finite-difference modeling based on exploding reflector concept (Figure 1b). Synthetic data replicates damaging scattering distortions observed on real data (Bakulin et al., 2020).

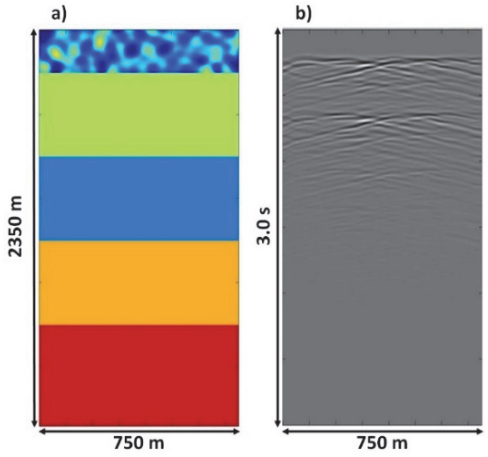

Figure 1: (a) True model of the complex near surface simulated as a fixed realization of the clutter with the spatial correlation length 35 m, mean velocity value 2000 m/s, and standard deviation of velocity 400 m/s. (b) Zero-offset data computed in the true model from (a).

Using the true model, we compute the ideal image result as a model reflectivity convolved with source impulse (Figure 2a). The actual reverse-time migration (RTM) of zero-offset data in the true clutter model is shown in Figure 2a. It possesses many imaging artifacts in addition to true subsurface reflectors. We use the ideal image as the exact reference solution and the image in the true clutter model as the best achievable result for benchmarking purposes.

To apply statistical imaging with path summation, we need a practical recipe to generate an ensemble of possible models. We assume that conventional seismic velocity model building would provide a smooth background or "tomographic" model (Figure 3a) approximating the true model but lacking many smaller details. We further assume without proof, that perturbations between background and true model are also described with Gaussian distribution and we can estimate two parameters of the distribution directly from the data. In this study, we keep the correlation length at 35 m, while reducing the standard deviation to 257 m/s (estimated here based on the standard deviation between smooth "tomographic" and the true clutter models). Using statistical parameters above allows efficient generation of an

ensemble of models for path summation. Figure 3b shows one of the model realizations.

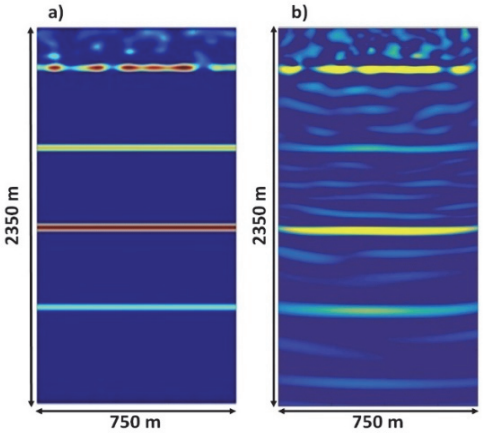

Figure 2: (a) True model reflectivity used an ideal image reference. (b) Zero-offset RTM image in the true clutter model as best achievable migrated image.

Finally, we applied the path summation approach. In this instance, 100 distinct model realizations were generated. Zero-offset RTM migration was performed for all of them to generate 100 different images. First, these images were simply stacked, and then weighted path summation was used according to equation (1). Weights (2) were created based on spatial frequency focusing measure (4). In general, migration result for a smooth clutter model or any realizations provides defocused images (Figures 4a, 4b).

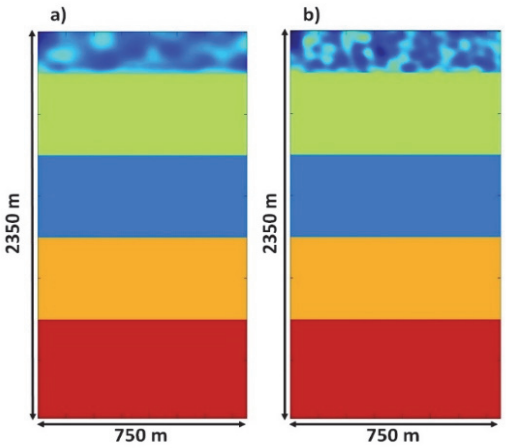

Figure 3: (a) Smooth background model of the true clutter assumed to be recovered during conventional velocity model building; (b) Single realization of the model from the statistical ensemble of models generated by introducing Gaussian perturbations to a smooth model from (a). Correlation length of 35 m and standard deviation of 257 m/s are used for Gaussian perturabtions.

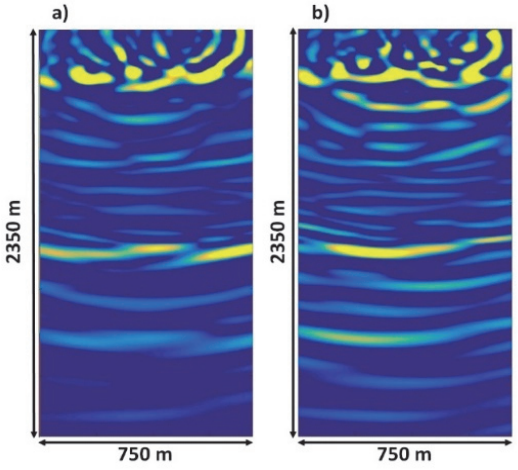

Figure 4: Zero-offset images obtained with different velocity models: (a) smooth background moded shown in Figure 3a; (b) single realization from the clutter ensemble (Figure 3b) used in statistical imaging.

Only some parts of the reflected interfaces are migrated properly. However, when we do even a simple summation, the stacked image provides reflected events in most of the area (Figure 5a). If we perform weighted image summation, then the result becomes better focused and less noisy than the simple stack (Figure 5b). The weighted image is closer to the ideal result (Figure 2a) and appears even less noisy than the migration in the true model (Figures 2b). Because we perform the migration with different models of the same data, we can generate an analog of common-image gather

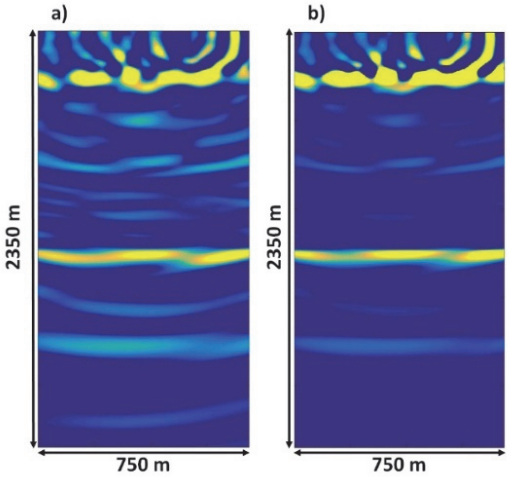

Figure 5: Statistical images with path summation using: (a) simple stack; (b) weighted stack.

(CIG) of RTM zero-offset migration with respect to the model realizations (Figure 6). One can observe that such raw

CIGs do not provide flat events at the reflector position (Figures 6a). They are scattered because of different perturbations in clutter realizations. However, when the weight based on the focusing measure is applied, the corresponding CIGs become more flattened and less perturbed (Figures 6b). Visually one can observe that a weighted image stack provides a better result than a simple image stack. Also, a weighted image stack looks less noisy than a simple image stack. In addition, it appears to contain fewer artifacts than the image in the true clutter model. To compare image quality quantitatively, we compute two metrics: signal-to-noise ratio (SNR) and correlation coefficient. An ideal reflectivity image (Figure 2a) is used as a signal for both metrics. SNR is computed over the entire image, and its mean value is reported (Bakulin et al., 2021). Table 1 summarizes both metrics for all considered images.

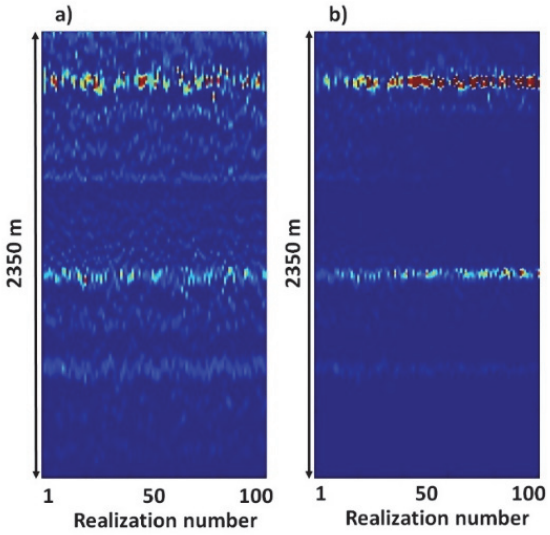

Figure 6: (a) Common-image gather of zero-offset migration with respect to the model realizations at $x=125\ m$. (b) Same as (a) but after applying appropriate weights.

Table 1 confirms that an image with the true clutter model is the best achievable solution among all images. However, visually, it appears noisier than the statistical images with path summation. Furthermore, each statistical image provides better quality than images obtained with the background model or single realization. Finally, metrics for weighted stack show measurable improvement compared to simple image stack.

	Signal-to-noise ratio	Correlation coefficient
Image in the exact model	**3.5 dB**	**0.75**
Image in the smooth background model	**-1.7 dB**	**0.06**
Image in one realization	**-2.5 dB**	**0.18**
Statistical image (simple stack)	**-0.7 dB**	**0.40**
Statistical image (weighted stack)	**1.3 dB**	**0.51**

Table 1: Assessment of image quality using Signal-to-Noise Ratio and correlation coefficient. The true model reflectivity (Figure 2a) is used as a "ground truth" for computing both metrics.

Conclusions

We apply statistical imaging with path summation to the synthetic land data with complex near surface. We represent near surface as a random clutter model with Gaussian heterogeneity distribution. We show that near-surface clutter destroys reflection images if it is not taken into account properly. Migration with the exact velocity model of the clutter recovers reflections (albeit with artifacts). However, such a model is not achievable in practice. Images using conventionally recoverable smoothed background model are substantially compromised. Statistical imaging can significantly improve and recover the reflectors provided statistical parameters for generating velocity realizations are properly guessed or estimated. Future studies should evaluate the sensitivity of path-summation imaging to the accuracy of statistical parameters used to characterize random heterogeneity. In addition, geological consideration can be invoked to evaluate plausible statistical properties describing near-surface geology. Leveraging advances in acoustics, estimating clutter parameters in a heterogeneous initial model should be feasible to create appropriate realizations required for the path summation approach. It is also clear that this topic also has a relationship to uncertainty quantification of the cluttered model.

Acknowledgments

The authors are grateful to Prof. Evgeny Landa for the inspiring discussions and introduction to the idea of path-integral imaging in cluttered media.

REFERENCES

Bakulin, A., D. Neklyudov, and I. Silvestrov, 2019, Importance of phase guides from beamformed data for processing multi-channel data in highly scattering media: Journal of Acoustical Society of America — Express Letters, **84**, D11–D23, doi: https://doi.org/10.1121/10.0001330.

Bakulin, A., I. Silvestrov, and M. Protasov, 2021, Quality control of 3D prestack land seismic data with a focus on data enhancement: 1st International Meeting for Applied Geoscience & Energy, SEG/AAPG, Expanded Abstracts, 2929–2934, doi: https://doi.org/10.1190/segam2021-3576612.1.

Borcea, L., G. Papanicolaou, and C. Tsogka, 2003, Theory and applications of time reversal and interferometric imaging: Inverse Problems, **19**, S139–S164, doi: https://doi.org/10.1088/0266-5611/19/6/058.

Burnett, W., S. Fomel, and R. Bansal, 2011, Diffraction velocity analysis by path-integral seismic imaging: 81st Annual International Meeting, SEG, Expanded Abstracts, 3898–3902.

Decker, L., and S. Fomel, 2019, Path-integral seismic diffraction imaging with probability weights: 89th Annual International Meeting, SEG, Expanded Abstracts, 4231–4235, doi: https://doi.org/10.1190/segam2019-3215424.1.

Eskicioglu, A. M., and P. S. Fisher, 2020, Image quality measures and their performance: IEEE Transactions on Communications, **85**, M85–M95, doi: https://doi.org/10.1109/26.477498.

Ikelle, L. T., S. K. Yung, and F. Daube, 1993, 2-D random media with ellipsoidal autocorrelation functions: Geophysics, **58**, 1359–1372, doi: https://doi.org/10.1190/1.1443518.

Keydar, S., and V. Shtivelman, 2020, Imaging zero-offset sections using multipath summation: First Break, **85**, KS149–KS160, doi: https://doi.org/10.3997/1365-2397.2005016.

Landa, E., 2004, Imaging without a velocity model using path summation approach: 74th Annual International Meeting, SEG, Expanded Abstracts, 1016–1019.

Landa, E., S. Fomel, and T. J. Moser, 2006, Path-integral seismic imaging: Geophysical Prospecting, **54**, 491–503, doi: https://doi.org/10.1111/j.1365-2478.2006.00552.x.

Landa, E., M. Reshef, and V. Khaidukov, 2005, Imaging without a velocity model using path-summation approach: This time in depth: 67th Annual International Conference and Exhibition, EAGE, Extended Abstracts, P011, doi: https://doi.org/10.3997/2214-4609-pdb.1.P011.

Merzlikin, D., and S. Fomel, 2015, An efficient workflow for path-integral imaging of seismic diffractions: 85th Annual International Meeting, SEG, Expanded Abstracts, 4096–4100, doi: https://doi.org/10.1190/segam2015-5849464.1.

Pertuz, S., D. Puig, and M. Garcia, 2020, Analysis of focus measure operators for shape-from-focus: Pattern Recognition, **85**, KS89–KS99.

Protasov, M., D. Kolyukhin, S. Rostomyan, and E. Landa, 2017, Subsalt imaging in the presence of salt-body uncertainty: The Leading Edge, **36**, 146–150, doi: https://doi.org/10.1190/tle36020146.1.

Sava, P., and O. Poliannikov, 2008, Interferometric imaging condition for wave-equation migration: Geophysics, **73**, no. 2, S47–S61, doi: https://doi.org/10.1190/1.2838043.

Schleicher, J., and J. C. Costa, 2009, Migration velocity analysis by double path-integral migration: Geophysics, **74**, no. 6, WCA225–WCA231, doi: https://doi.org/10.1190/1.3162482.

Xie, X.-B., H. Ning, and B. Chen, 2016, How scatterings from small-scale near-surface heterogeneities affecting seismic data and the quality of depth image, analysis based on seismic resolution: 86th Annual International Meeting, SEG, Expanded Abstracts, 4278–4282, doi: https://doi.org/10.1190/segam2016-13780223.1.

Yilmaz, Ö., 2018, Circumventing velocity uncertainty in imaging complex structures: The Leading Edge, **37**, 14–18, doi: https://doi.org/10.1190/tle37010014.1.